

1 **Full title:** Coordinated periodic expression of the imprinted network genes in the hair follicle growth
2 cycle.

3 **Short title:** Imprinted network genes in hair follicle cycling

4

5 **Authors:**

6 Alexandra K. Marr*¹, Sabri Boughorbel¹, Aouatef I. Chouchane¹ and Tomoshige Kino¹

7

8 **Affiliation:**

9 Sidra Medicine

10 Research Branch

11 Doha , Qatar

12

13 **E-mail addresses:**

14 Alexandra K. Marr: amarr@sidra.org (AKM)

15 Sabri Boughorbel: sboughorbel@sidra.org

16 Aouatef I. Chouchane: achouchane@sidra.org

17 Tomoshige Kino: kinot1025@gmail.com

18

19 *corresponding author

20 Abstract

21 Imprinted genes play a critical role in the proliferation and differentiation of embryonic cells and
22 somatic stem cells. They also participate in the development of a wide spectrum of clinical
23 manifestations when they are dysregulated. In this study, we analyzed expression profiles of the
24 network-forming 16 imprinted genes (imprinted gene network: IGN) in three phases of the hair follicle
25 growth cycle by analyzing publicly available datasets deposited in the Gene Expression Omnibus (GEO).
26 We found elevated expression of IGN genes including *H19* in the telogen quiescent phase compared to
27 the anagen proliferative and catagen regression phases in the transcriptomic dataset created from the
28 mouse skin biopsy samples. Our findings suggest a novel role of the 16 IGN genes in the regulation of
29 the hair follicle growth cycle, that manifests possibly through altering the transition between
30 proliferation, quiescence and/or differentiation of the follicular stem cells.

31

32

33 **Keywords:** follicular stem cells, genomic imprinting, growth cycle, skin hair follicle, telogen phase

34 Introduction

35 Genomic imprinting is an epigenetic regulatory mechanism that confers the expression of selected
36 genes from one parental allele, and thus, transfer of its effects to descendants does not follow the
37 classic Mendelian pattern (1). Genomic imprinting is established in the parental germline cells, and is
38 maintained throughout mitotic cell divisions in somatic cells (2). Thus far, 85 and 95 murine imprinted
39 genes are reported in the COXPRESdb and the Gemma database, respectively (1). The process of gene
40 imprinting involves coordinated DNA and histone methylation, whereas the mechanisms underlying its
41 selective targeting to a particular set of genes is largely unknown (3). Altered expression of imprinted
42 genes has been associated with the development of various pathological conditions in humans,
43 including obesity, diabetes mellitus, muscular dystrophy, mental disability and neoplasms (1).

44 Imprinted genes are composed of functionally distinct members, but most are involved in controlling the
45 transition of cells between their quiescent, proliferation and/or differentiation states (1). These genes
46 cooperatively participate in the regulation of specific biological pathways by forming a gene cluster
47 called the imprinted gene network (IGN), which is further divided into three subgroups based on their
48 functional and regulatory connectivity (1). One of these subgroups is comprised of 16 imprinted genes
49 [namely Cyclin Dependent Kinase Inhibitor 1C (*Cdkn1c*), Decorin (*Dcn*), Delta Like Non-Canonical Notch
50 Ligand 1 (*Dlk1*), Glycine Amidinotransferase (*Gatm*), *GNAS* Complex Locus (*Gnas*), Growth Factor
51 Receptor Bound Protein 10 (*Grb10*), Imprinted Maternally Expressed Transcript (*H19*), Insulin Like
52 Growth Factor 2 (*Igf2*), Insulin Like Growth Factor 2 Receptor (*Igf2r*), Maternally Expressed 3 (*Meg3*),
53 Mesoderm Specific Transcript (*Mest*), Necdin (*Ndn*), Paternally Expressed 3 (*Peg3*), PLAGL1 Like Zink
54 Finger 1 (*Plagl1/Zac1*), Sarcoglycan Epsilon (*Sgce*), Solute Carrier Family 38 Member 4 (*Slc38a4*)], all of
55 which are known to be involved in the control of embryonic, fetal and/or postnatal growth (3). Their
56 targeted deletion also develops over-growth phenotypes in mice (4). Expression of this subset of 16

57 imprinted genes (hereafter called the IGN genes) is generally elevated at the transition from cell
58 proliferation to quiescence or differentiation, as observed during the fibroblast cell cycle withdrawal,
59 adipogenesis and muscle regeneration (1). It was shown that the *Plag1/Zac1* influences the expression
60 of some member genes (*Igf2*, *H19*, *Cdkn1c* and *Dlk1*) (3), while H19 long non-coding RNA fine-tunes the
61 expression of other genes (4). These pieces of evidence suggest that biological input from upstream
62 signaling pathways to one or some of the network genes triggers coordinated expression of other IGN
63 genes by activating their mutual regulatory cascades, which ultimately influences the transition of cells
64 in which they are expressed from proliferation to quiescence or differentiation state (or *vice versa*) (4).

65 Hair growth and renewal are organized by the cycling activity of the hair follicles. During their life span,
66 hairs undergo the process of proliferation, degeneration and regeneration in concert with the activation
67 and quiescence of the epidermal stem cells located in the bulge of the hair follicles (5, 6). The cyclical
68 activity of hair follicles is divided into three phases, referred to as the anagen (growth), catagen
69 (regression), and the telogen (resting) phases (7). The follicular stem cells are maintained in a quiescent
70 state during the telogen phase. Once they receive the activating signals from upstream regulatory
71 systems, they initiate a new round of hair growth (anagen phase) (6, 8, 9). After the active growth
72 phase, proliferating matrix cells of the hair follicles are induced to undergo coordinated apoptosis
73 (catagen phase) (7). Following catagen, the hair follicles move eventually to the telogen phase in which
74 hairs are no longer produced due to inactivation of the follicular stem cells (7).

75 The aim of this study was to examine the involvement of the IGN genes in the process of hair cycling
76 organized in hair follicles by analyzing publicly available data resources. We identified one dataset with
77 transcriptome profiles of the different cycling stages of hair follicles in mouse skin. Using *in silico* data
78 analysis, we found that the IGN genes show characteristic expression patterns with an elevated
79 expression in the telogen phase compared to the anagen phase of the hair follicles. We provide
80 evidence that the IGN genes play important roles in the skin/hair follicle biology in after-birth life in

81 addition to their well-known activity during embryonic/fetal growth. Our results also suggest the
82 possibility that these genes are involved in certain pathological processes of hair follicles.

83

84 Materials and Methods

85 To identify the publicly available data in which our genes of interest are differentially expressed, a
86 specific query or single keyword (see Results section) was used in the GEO Profiles database, which
87 stores gene expression data derived from the curated GEO DataSets (10). Identified transcriptomic
88 datasets present the expression levels of the selected gene across all samples within the dataset. We
89 then curated all filtered datasets for differential expression of our genes of interest. To compare gene
90 expression profiles in two or more groups of samples in a dataset, the interactive web tool GEO2R was
91 used (11). One-way ANOVA analysis on quantile normalized data with Bonferroni post-testing was used
92 for multiple comparisons, whereas two-tailed t-test was performed on the quantile normalized data for
93 two group comparisons.

94

95 Results

96 Identification of datasets harboring differential expression of H19 in skin

97 To identify publicly available datasets in which imprinted genes of the IGN could be examined in the
98 skin, we queried for 'H19[*gene symbol*] AND skin' in the NCBI GEO Profiles (10). We selected *H19* as a
99 representative for imprinted genes in this initial search, as it is known to influence the expression of
100 several other imprinted genes in IGN (4). This search revealed 156 datasets, which were manually
101 curated for differential expression of *H19* across all samples within a dataset, based on the visual gene

102 expression level displayed in the GEO Profiles. Using this strategy, we finally identified one dataset
103 (GSE11186 (12)), which contains transcriptomic profiles of the different stages of the first and the
104 second synchronized natural and a depilation-induced growth cycles of hair follicles from mouse skin
105 biopsies. In this dataset, H19 expression is significantly elevated in the first telogen phase (day 23) and
106 second telogen phase (day 44) compared to the anagen (day 27) or catagen (days 37 and 39) phases (Fig
107 1).

108 **Fig 1. Time-course profile of H19 expression during the synchronized first- and second postnatal hair**
109 **growth cycle.** Values shown are quantile normalized absolute expression data from GSE11186 for
110 telogen (day 23, n=2), mid anagen (day 27, n=3), catagen (day 37 and day 39, n=6) and telogen (day 44,
111 n=3). P-value shown in the upper right corner of the graph was determined by ordinary one-way ANOVA
112 corrected for multiple comparisons using Bonferroni test. n.s.: not statistically significant, *: $p \leq 0.05$,
113 ****: $p \leq 0.0001$

114

115 **IGN gene expression is elevated during the telogen phase of hair follicle growth cycle**

116 A previous report demonstrated that H19 forms an IGN together with 15 additional co-regulated
117 imprinted genes (3). Thus, we examined the expression of these 15 IGN genes associated with H19 in the
118 identified dataset. Using GEO2R, we identified differential expression of the 16 imprinted genes (*Cdkn1c*,
119 *Dcn*, *Dlk1*, *Gatm*, *Gnas*, *Grb10*, *H19*, *Igf2*, *Igf2r*, *Meg3*, *Mest*, *Ndn*, *Peg3*, *Plagl1*, *Sgce*, *Slc38a4*) across all
120 experimental conditions in the dataset by comparing the quantile normalized data of GSE11186.

121 Notably, we observed a significant difference in the mean expression ratio of all 16 IGN member genes
122 when comparing telogen phase (day 23) over catagen phase (day 37 and day 39), which was not the
123 case in the comparison of the mid anagen phase (day 27) over the catagen phase (day 37 and day 39)
124 (Fig 2A).

125 **Fig 2. Expression of all 16 IGN genes in the telogen and the anagen phases.** (A) The fold expression
126 values of all pooled 16 IGN genes identified in the telogen phase (T, day 23) and the anagen phase (A,
127 day 27) were normalized to those of the catagen phase (C, day 37 and day 39) in the dataset GSE11186.
128 T/C- and A/C values that correspond to the same gene are connected with a line. The A/C fold value is
129 smaller than the T/C fold value for all IGN genes except for *Dcn* and *Igf2r* (marked in red). Statistical
130 comparison of T/C- and A/C values was made using a paired Student t test, **: $p < 0.001$. (B) Dot plot
131 showing the absolute expression (after quantile normalization) of the IGN genes and control genes in
132 telogen (day 23) and anagen (day 27) from GSE11186. Each dot (telogen: blue and anagen: red)
133 corresponds to a subject from dataset GSE11186. IGN genes tend to be higher expressed in telogen
134 compared to anagen. Known telogen activated genes (*Ar*, *Esr1*, *Lhx2*, *Nr1d1*, *Sox18*, *Stat3*) and telogen
135 repressed genes (*Elf5*, *Foxn1*, *Grhl1*, *Lef1*, *Msx2*, *Vdr*) (12) were used as controls.

136
137 Next, we examined the absolute expression levels of each IGN gene separately in telogen (day 23) and
138 mid anagen (day 27) from the synchronized second postnatal hair growth cycle from dataset GSE11186.
139 For comparison, we also examined the absolute expression of six known telogen-activated genes (*Ar*,
140 *Esr1*, *Lhx2*, *Nr1d1*, *Sox18*, *Stat3*), and six known telogen-repressed genes (*Elf5*, *Foxn1*, *Grhl1*, *Lef1*, *Msx2*,
141 *Vdr*) (12). Again, we observed that IGN gene expression was elevated in telogen compared to mid
142 anagen, with some of the IGN genes (i.e. *H19*, *Gnas*, *Meg3*) even expressed at higher levels than the
143 known telogen-activated genes (Fig 2B).

144
145 **Most IGN genes are periodically expressed, thus they are considered as hair cycle-regulated genes**

146 To assess whether the IGN genes are hair cycle-regulated, we took advantage of a public available
147 dataset that was obtained after processing mRNA microarray data from mouse skin at eight time points

148 corresponding to the first synchronously (days 1, 6 and 14: anagen, day 17: catagen, day 23: telogen)
149 and the asynchronously (9th week, 5th month, 1st year) postnatal hair cycling, with the latter three
150 time point samples containing skin patches in different phases of the hair-growth cycle (13). After
151 excluding genes that were not expressed in the mouse skin and applying a computational approach
152 including replicate variance analysis (*F* test), Lin *et al.* identified a dataset of 2,461 probe sets
153 corresponding to 2,289 potential hair cycle-associated genes (hereafter called ‘Lin1-dataset’) (13). The *P*-
154 value cut-off for the *F* test was set previously to 0.05, as it was found that > 80% of known hair cycle-
155 dependent expressed genes had a *P*-value of < 0.05 using this computational approach (13). As the pool
156 of these 2,289 hair cycle-associated genes are restricted to protein-coding genes, we included only the
157 14 protein-coding IGN genes (*Igf2*, *Cdkn1c*, *Dcn*, *Dlk1*, *Gatm*, *Gnas*, *Grb10*, *Igf2r*, *Ndn*, *Mest*, *Peg3*, *Plagl1*,
158 *Sgce* and *Slc38a4*) in our analysis and excluded the two non-coding RNA IGN genes (*H19* and *Meg3*). We
159 identified ten IGN genes (*Cdkn1c*, *Dcn*, *Dlk1*, *Gatm*, *Gnas*, *Igf2r*, *Ndn*, *Peg3*, *Sgce*, *Slc38a4*), corresponding
160 to 71% of all protein-coding IGN genes, among the pool of 2,461 probe sets categorized as periodically
161 expressed, hair cycle-regulated genes in the mouse dorsal skin (Fig 3A). The Lin1-dataset had been
162 previously characterized by cluster analysis and was divided into three general profile patterns (‘anti-
163 hair growth’-, ‘hair growth’-, and ‘catagen-related’ pattern), and further subdivided into 30 clusters of
164 co-expressed genes which differed by their expression peaks at different stages of the hair growth cycle
165 (13). Seven of our identified hair cycle-associated IGN genes (*Cdkn1c*, *Dlk1*, *Gnas*, *Peg3*, *Gatm*, *Ndn*,
166 *Slc38a4*) fell into the ‘anti-hair growth’ category and showed a decline in expression levels during
167 anagen. One IGN gene (*Igf2r*) fell into the ‘hair growth’ pattern with peak expression at early anagen. On
168 the contrary, *Sgce* was categorized as ‘catagen-related’ gene with a drop in expression level at catagen
169 and finally, one IGN gene (*Dcn*) belongs to a gene cluster that does not fall into the three main profile
170 patterns (Table 1).

171 **Fig 3. Most GN genes are periodically expressed, hair-cycle regulated genes. (A)** Venn Diagram
 172 illustrating that 71% of protein coding IGN genes (10 out of 14) are hair cycle-regulated. The ten protein
 173 coding-, hair cycle-regulated IGN genes identified are *Cdkn1c*, *Dcn*, *Dlk1*, *Gatm*, *Gnas*, *Igf2r*, *Ndn*, *Peg3*,
 174 *Sgce*, and *Slc38a4*. **(B)** Time course profiles of hair cycle regulated IGN genes during hair follicle cycling.
 175 Shown are the normalized expression levels of eight hair cycle regulated IGN genes (*Igf2*, *Cdkn1c*, *Dcn*,
 176 *Dlk1*, *Gnas*, *Mest*, *Peg3*, *Plagl1*) in red, eleven control genes (telogen upregulated genes (12): *Dbp*, *Tef*,
 177 *Nr1d1*, *Per1*, *Per2*, and anagen/catagen upregulated genes (12): *Dlx3*, *Elf5*, *Foxn1*, *Foxq1*, *Hoxc13*, and
 178 *Ovol1*) in black. Normalized gene expression values are provided in supplemental table S1 from (12). **(C)**
 179 Time-course profile of *Meg3* expression during the synchronized first- and second postnatal hair growth
 180 cycle. Values shown are quantile normalized absolute expression data from GSE11186 for telogen (day
 181 23, n=2), mid anagen (day 27, n=3), catagen (day 37 and day 39, n=6) and telogen (day 44, n=3). P-value
 182 shown in the upper right corner of the graph was determined by ordinary one-way ANOVA corrected for
 183 multiple comparisons using Bonferroni test. n.s.: not statistically significant, *: $p \leq 0.05$, ****: $p \leq 0.0001$.

184

185 **Table 1. Potential hair cycle-regulated IGN genes (identified in Lin1-dataset)**

Gene Symbol	Gene name	P-value*	cluster description*
<i>Cdkn1c</i> **	cyclin-dependent kinase inhibitor 1C (P57)	0.0004	anti-hair growth pattern with decline expression level during anagen
<i>Dcn</i> **	Decorin	0.0392	does not fall into any of the three main profile patterns
<i>Dlk1</i> **	delta-like 1 homolog (Drosophila)	0.0166	anti-hair growth pattern with decline expression level during anagen
<i>Gatm</i>	glycine amidinotransferase (L-arginine:glycine amidinotransferase)	0.0009	anti-hair growth pattern with decline expression level during anagen
<i>Gnas</i> **	GNAS (guanine nucleotide binding protein, alpha stimulating) complex locus	0.0040	anti-hair growth pattern with decline expression level during anagen
<i>Igf2R</i>	insulin-like growth factor 2 receptor	0.0004	hair growth pattern including genes that peak at early anagen
<i>Ndn</i>	necdin	0.0171	anti-hair growth pattern with decline expression level during anagen
<i>Peg3</i> **	paternally expressed 3	0.0001	anti-hair growth pattern with decline expression level during anagen

<i>Sgce</i>	sarcoglycan, epsilon	0.0117	catagen-related expression patterns with drop in expression level at catagen
<i>Slc38a4</i>	solute carrier family 38, member 4	0.0013	anti-hair growth pattern with decline expression level during anagen

186 * Defined by Lin *et al.* (13)

187 ** Gene was independently identified as potential hair cycle-regulated gene in Lin2-dataset (see Table 2)

188

189 Next, we analyzed an independent, published dataset (hereafter called 'Lin2-dataset') comprising a set
190 of previously identified 6,393 mRNA probe sets (corresponding to 4,704 genes) (12). This pool of 4,704
191 genes was identified by Lin *et al.* by processing expression data obtained from mRNA profiles of the
192 mouse dorsal skin at multiple time points during: 1) the postnatal completion of hair follicle
193 morphogenesis, including the first catagen and telogen; 2) the synchronized second postnatal hair
194 growth cycle; and 3) a depilation-induced hair growth cycle (12). By applying a matrix model, 8433
195 periodically expressed probe sets (6,010 genes) were identified, of which 2,040 probe sets (1,306 genes)
196 were excluded from this subset since these genes changed their expression due to the cell-type
197 composition that occur in the skin during the hair follicle cycling (such as cornified cells, suprabasal cells,
198 mesenchymal cells and myocytes) (12). The final set of 6,393 probe sets (4,704 genes, Lin2-dataset)
199 exhibited periodic expression patterns that cannot be explained by cell-type specific alterations of the
200 skin that occur during the hair follicle cycling and were thus defined as hair cycle-regulated genes (12).
201 Similar to the Lin1-dataset, this set of 4,704 hair cycle-regulated genes are restricted to protein-coding
202 genes. Thus, we included only the 14 protein-coding IGN genes in our analysis, excluding the two non-
203 coding RNA IGN genes. We identified eight IGN genes (*Igf2*, *Cdkn1c*, *Dcn*, *Dlk1*, *Gnas*, *Mest*, *Peg3*, *Plagl1*)
204 (corresponding to 57% of all protein-coding IGN genes) among the pool of 6,347 probe sets of the Lin2-
205 dataset that were categorized as periodically expressed, hair cycle-regulated genes in the mouse dorsal
206 skin (Table 2) (12). 3,180 genes from the Lin2-dataset were grouped earlier according to their
207 expression peak during the hair growth cycle with 1,169 genes in early anagen, 1,017 genes in mid

208 anagen, 243 genes in late anagen, 208 genes in early catagen, 253 genes in mid catagen and 290 genes
 209 in telogen (12). The eight IGN genes identified in this study being among the hair cycle-regulated genes
 210 of the Lin2-dataset were categorized as genes with expression peak in telogen (*Dcn*, *Gnas*) and early
 211 anagen (*Igf2*, *Cdkn1c*, *Dlk1*, *Mest*, *Peg3*, *PlagL1*) (Table 2). Furthermore, we examined the gene
 212 expression levels of the eight hair cycle-regulated IGN genes (listed in table 2) during the nine time
 213 points provided in the ‘Lin2-dataset’ (12). The gene expression levels of the eight hair cycle-regulated
 214 IGN genes show elevated gene expression profiles in telogen and early anagen compared to mid/late
 215 anagen and catagen (Fig 3B), similar to *Dbp*, *Nr1d1*, *Per1*, *Per2*, and *Tef* which were shown earlier to
 216 have prominent expression during telogen (12). In contrary, their expression differs from *Dlx3*, *Elf5*,
 217 *Foxn1*, *Foxq1*, *Hoxc13*, and *Ovol1*, a group of transcriptional regulators that have an expression peak
 218 from mid anagen to late catagen (12).

219 **Table 2. Potential hair cycle-regulated IGN genes (identified in Lin2-dataset)**

Gene Symbol	Gene name	cluster description*
<i>Cdkn1c</i> **	cyclin-dependent kinase inhibitor 1C (P57)	Expression peaks at early anagen
<i>Dcn</i> **	Decorin	Expression peaks at telogen
<i>Dlk1</i> **	delta-like 1 homolog (Drosophila)	Expression peaks at early anagen
<i>Gnas</i> **	GNAS (guanine nucleotide binding protein, alpha stimulating) complex locus	Expression peaks at telogen
<i>Igf2</i>	insulin like growth factor 2	Expression peaks at early anagen
<i>Mest</i>	mesoderm specific transcript	Expression peaks at early anagen
<i>Peg3</i> **	paternally expressed 3	Expression peaks at early anagen
<i>Plag1</i>	PLAG1 like zinc finger 1	Expression peaks at early anagen

220 * Defined by Lin *et al.* (12)

221 ** Gene was also identified as potential hair cycle-regulated gene in Lin1-dataset (see Table 1)

222

223 Finally, as non-coding RNA genes in general were not included in the Lin1- and Lin2-datasets, we
 224 established the time course profile of *Meg3* expression during telogen (day 23), mid anagen (day 27),
 225 catagen (day 37 and day 39) as well as telogen (day 44) with expression values provided in dataset
 226 GSE11186 (12). In this analysis we identified a periodic expression pattern of the non-coding RNA *Meg3*

227 during the hair cycle with significantly reduced expression levels during mid anagen and catagen (Fig
228 3C), similar as we showed in this study for the non-coding IGN gene H19 (Fig 1).

229

230 Discussion

231 The 16 IGN genes examined in this study are known to play important roles in the embryonic
232 development (3, 14). However, involvement of this particular set of imprinted genes in other biological
233 processes and regulatory mechanisms associated with these genes were largely unknown. Here we
234 report a coordinated elevation in the telogen and early anagen phase compared to the mid anagen
235 phase of the hair follicle growth cycle. Thus, the majority of the protein-coding IGN genes is considered
236 as the hair cycle-regulated genes. Hair cycle-associated changes in the expression of members of the
237 IGN genes have not been previously described. Thus, our results emphasize the importance of these
238 imprinted genes for the transition from cell quiescence (telogen phase) to proliferation (anagen phase)
239 possibly by acting as negative regulatory factors, and further suggest their vital roles in skin/hair
240 homeostasis (15). This is consistent with previous reports indicating the involvement of IGN genes in
241 muscle regeneration and haematopoietic stem cell biology (3, 14).

242 The IGN genes we examined in this study are downregulated postnatally, but are continuously
243 expressed in pluripotent stem cells and/or progenitor cells of the hematopoietic system, skin and
244 skeletal muscles with a significant lower expression levels in their differentiated progeny (15). Somatic
245 stem cells, such as haematopoietic stem cells, epidermal stem cells and satellite cells of the skeletal
246 muscles are generally considered to be quiescent, dividing infrequently, but are driven into active
247 proliferation/differentiation cycles upon tissue regeneration or for self-renewal (15). Our results suggest
248 a periodic expression cycle of the IGN genes during the follicular growth cycle with zenith in the telogen

249 and early anagen phase and nadir in the mid anagen and catagen phase, which is in agreement with the
250 consensus that hair follicle stem cells receive activating or inhibitory signals at distinct stages of the hair
251 growth cycle, allowing them to either remain quiescent or become proliferative (16). During the
252 transition from the telogen to the anagen phase, biological signals from the dermal papilla stimulate the
253 quiescent follicular stem cells to proliferate (17). At the same time, melanocytes are also activated,
254 supplying multiplied progeny to the hair matrix, where most of them mature into differentiated
255 melanocytes (18, 19). As most of the IGN genes are known as tumor suppressors, it is likely that the
256 decrease in the expression of these IGN genes from the telogen to the anagen phase triggers the
257 biological cascades stimulating cell proliferation (20-30). Further, the dysregulation of IGN genes might
258 participate in the autonomic proliferation of their transformed cells observed in malignant melanoma,
259 and might be involved in certain congenital syndromes characterized by impaired hair growth cycles
260 such as the short anagen hair syndrome (31), or the synchronized pattern of scalp hair growth (32).

261

262 Acknowledgements

263 The authors would like to thank Dr. N. Marr for critically reading the manuscript.

264

265 Data availability

266 The datasets underlying the results are available in the NCBI GEO DataSets (GSE11186) at

267 ncbi.nlm.nih.gov/gds/ as well as in the supplemental material of (12) and of (13).

268

269 Competing interests

270 No competing interests were disclosed.

271

272 Grant information

273 The study was supported by Sidra Medicine Internal Research Fund to TK. The authors declared that no
274 grants were involved in supporting this work.

275

276 References

- 277 1. Al Adhami H, Evano B, Le Digarcher A, Gueydan C, Dubois E, Parrinello H, et al. A systems-level
278 approach to parental genomic imprinting: the imprinted gene network includes extracellular matrix
279 genes and regulates cell cycle exit and differentiation. *Genome Res.* 2015;25(3):353-67.
- 280 2. Wood AJ, Oakey RJ. Genomic imprinting in mammals: emerging themes and established
281 theories. *PLoS Genet.* 2006;2(11):e147.
- 282 3. Varrault A, Gueydan C, Delalbre A, Bellmann A, Houssami S, Aknin C, et al. Zac1 regulates an
283 imprinted gene network critically involved in the control of embryonic growth. *Dev Cell.* 2006;11(5):711-
284 22.
- 285 4. Gabory A, Ripoché MA, Le Digarcher A, Watrin F, Ziyat A, Forne T, et al. H19 acts as a trans
286 regulator of the imprinted gene network controlling growth in mice. *Development.* 2009;136(20):3413-
287 21.

- 288 5. Zhang X, Wang Y, Gao Y, Liu X, Bai T, Li M, et al. Maintenance of high proliferation and
289 multipotent potential of human hair follicle-derived mesenchymal stem cells by growth factors. *Int J Mol*
290 *Med*. 2013;31(4):913-21.
- 291 6. Leishman E, Howard JM, Garcia GE, Miao Q, Ku AT, Dekker JD, et al. Foxp1 maintains hair follicle
292 stem cell quiescence through regulation of Fgf18. *Development*. 2013;140(18):3809-18.
- 293 7. Alonso L, Fuchs E. The hair cycle. *J Cell Sci*. 2006;119(Pt 3):391-3.
- 294 8. Qiu W, Lei M, Zhou L, Bai X, Lai X, Yu Y, et al. Hair follicle stem cell proliferation, Akt and Wnt
295 signaling activation in TPA-induced hair regeneration. *Histochem Cell Biol*. 2017;147(6):749-58.
- 296 9. Kimura-Ueki M, Oda Y, Oki J, Komi-Kuramochi A, Honda E, Asada M, et al. Hair cycle resting
297 phase is regulated by cyclic epithelial FGF18 signaling. *J Invest Dermatol*. 2012;132(5):1338-45.
- 298 10. Leonardi C, Matheson R, Zachariae C, Cameron G, Li L, Edson-Heredia E, et al. Anti-interleukin-17
299 monoclonal antibody ixekizumab in chronic plaque psoriasis. *N Engl J Med*. 2012;366(13):1190-9.
- 300 11. Swindell WR, Johnston A, Carbajal S, Han G, Wohn C, Lu J, et al. Genome-wide expression
301 profiling of five mouse models identifies similarities and differences with human psoriasis. *PLoS One*.
302 2011;6(4):e18266.
- 303 12. Lin KK, Kumar V, Geyfman M, Chudova D, Ihler AT, Smyth P, et al. Circadian clock genes
304 contribute to the regulation of hair follicle cycling. *PLoS Genet*. 2009;5(7):e1000573.
- 305 13. Lin KK, Chudova D, Hatfield GW, Smyth P, Andersen B. Identification of hair cycle-associated
306 genes from time-course gene expression profile data by using replicate variance. *Proc Natl Acad Sci U S*
307 *A*. 2004;101(45):15955-60.
- 308 14. Piedrahita JA. The role of imprinted genes in fetal growth abnormalities. *Birth Defects Res A Clin*
309 *Mol Teratol*. 2011;91(8):682-92.
- 310 15. Berg JS, Lin KK, Sonnet C, Boles NC, Weksberg DC, Nguyen H, et al. Imprinted genes that regulate
311 early mammalian growth are coexpressed in somatic stem cells. *PLoS One*. 2011;6(10):e26410.

- 312 16. Lee J, Tumber T. Hairy tale of signaling in hair follicle development and cycling. *Semin Cell Dev*
313 *Biol.* 2012;23(8):906-16.
- 314 17. Gentile P, Scioli MG, Bielli A, Orlandi A, Cervelli V. Stem cells from human hair follicles: first
315 mechanical isolation for immediate autologous clinical use in androgenetic alopecia and hair loss. *Stem*
316 *Cell Investig.* 2017;4:58.
- 317 18. Nishimura EK, Jordan SA, Oshima H, Yoshida H, Osawa M, Moriyama M, et al. Dominant role of
318 the niche in melanocyte stem-cell fate determination. *Nature.* 2002;416(6883):854-60.
- 319 19. Nishimura EK, Granter SR, Fisher DE. Mechanisms of hair graying: incomplete melanocyte stem
320 cell maintenance in the niche. *Science.* 2005;307(5710):720-4.
- 321 20. Yoshimizu T, Miroglio A, Ripoche MA, Gabory A, Vernucci M, Riccio A, et al. The H19 locus acts in
322 vivo as a tumor suppressor. *Proc Natl Acad Sci U S A.* 2008;105(34):12417-22.
- 323 21. Yang H, Das P, Yu Y, Mao W, Wang Y, Baggerly K, et al. NDN is an imprinted tumor suppressor
324 gene that is downregulated in ovarian cancers through genetic and epigenetic mechanisms. *Oncotarget.*
325 2016;7(3):3018-32.
- 326 22. Piras G, El Kharroubi A, Kozlov S, Escalante-Alcalde D, Hernandez L, Copeland NG, et al. *Zac1*
327 (*Lot1*), a potential tumor suppressor gene, and the gene for epsilon-sarcoglycan are maternally
328 imprinted genes: identification by a subtractive screen of novel uniparental fibroblast lines. *Mol Cell*
329 *Biol.* 2000;20(9):3308-15.
- 330 23. Jarvinen TA, Prince S. Decorin: A Growth Factor Antagonist for Tumor Growth Inhibition. *Biomed*
331 *Res Int.* 2015;2015:654765.
- 332 24. Kawakami T, Chano T, Minami K, Okabe H, Okada Y, Okamoto K. Imprinted *DLK1* is a putative
333 tumor suppressor gene and inactivated by epimutation at the region upstream of *GTL2* in human renal
334 cell carcinoma. *Hum Mol Genet.* 2006;15(6):821-30.

- 335 25. Takahashi N, Yamaguchi E, Kawabata Y, Kono T. Deleting maternal Gtl2 leads to growth
336 enhancement and decreased expression of stem cell markers in teratoma. *J Reprod Dev.* 2015;61(1):7-
337 12.
- 338 26. Algar EM, Muscat A, Dagar V, Rickert C, Chow CW, Biegel JA, et al. Imprinted CDKN1C is a tumor
339 suppressor in rhabdoid tumor and activated by restoration of SMARCB1 and histone deacetylase
340 inhibitors. *PLoS One.* 2009;4(2):e4482.
- 341 27. Oka Y, Waterland RA, Killian JK, Nolan CM, Jang HS, Tohara K, et al. M6P/IGF2R tumor
342 suppressor gene mutated in hepatocellular carcinomas in Japan. *Hepatology.* 2002;35(5):1153-63.
- 343 28. Ross RJ, Weiner MM, Lin H. PIWI proteins and PIWI-interacting RNAs in the soma. *Nature.*
344 2014;505(7483):353-9.
- 345 29. Mroue R, Huang B, Braunstein S, Firestone AJ, Nakamura JL. Monoallelic loss of the imprinted
346 gene Grb10 promotes tumor formation in irradiated Nf1+/- mice. *PLoS Genet.* 2015;11(5):e1005235.
- 347 30. Feng W, Marquez RT, Lu Z, Liu J, Lu KH, Issa JP, et al. Imprinted tumor suppressor genes ARHI
348 and PEG3 are the most frequently down-regulated in human ovarian cancers by loss of heterozygosity
349 and promoter methylation. *Cancer.* 2008;112(7):1489-502.
- 350 31. Herskovitz I, de Sousa IC, Simon J, Tosti A. Short anagen hair syndrome. *Int J Trichology.*
351 2013;5(1):45-6.
- 352 32. Thai KE, Sinclair RD. Short anagen hair with persistent synchronized pattern of scalp hair growth.
353 *J Am Acad Dermatol.* 2003;49(5):949-51.

354

355

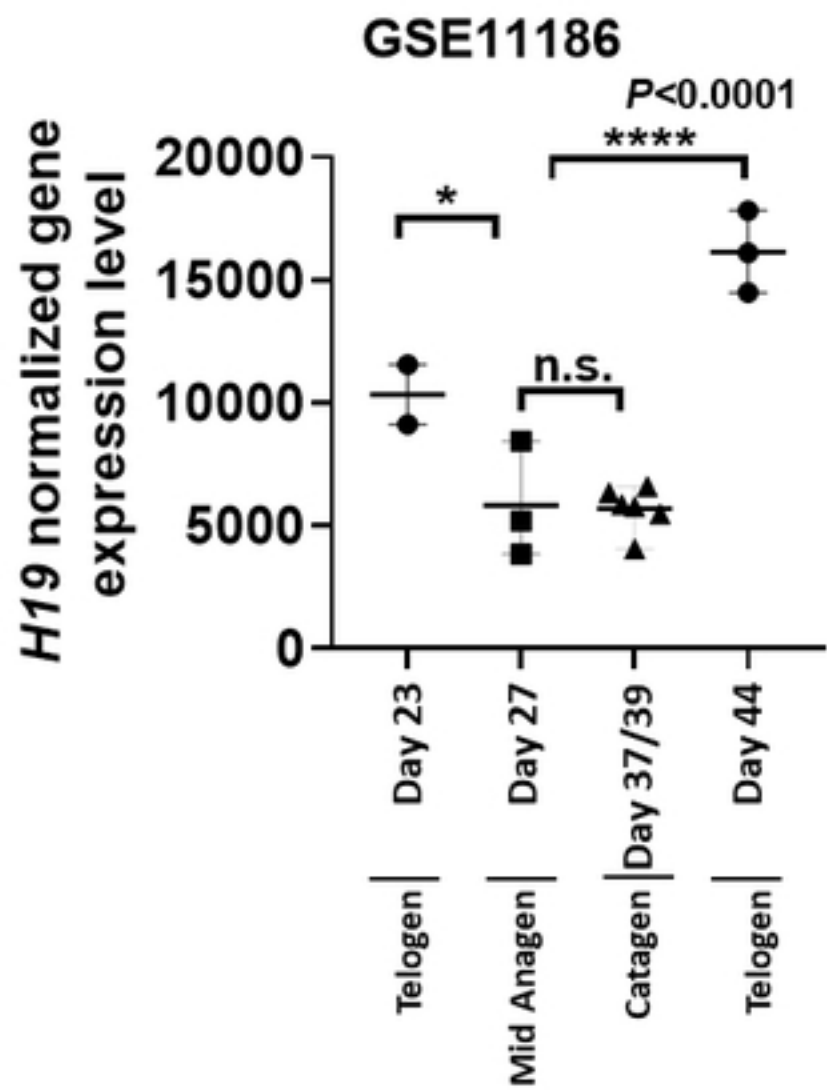


Figure 1

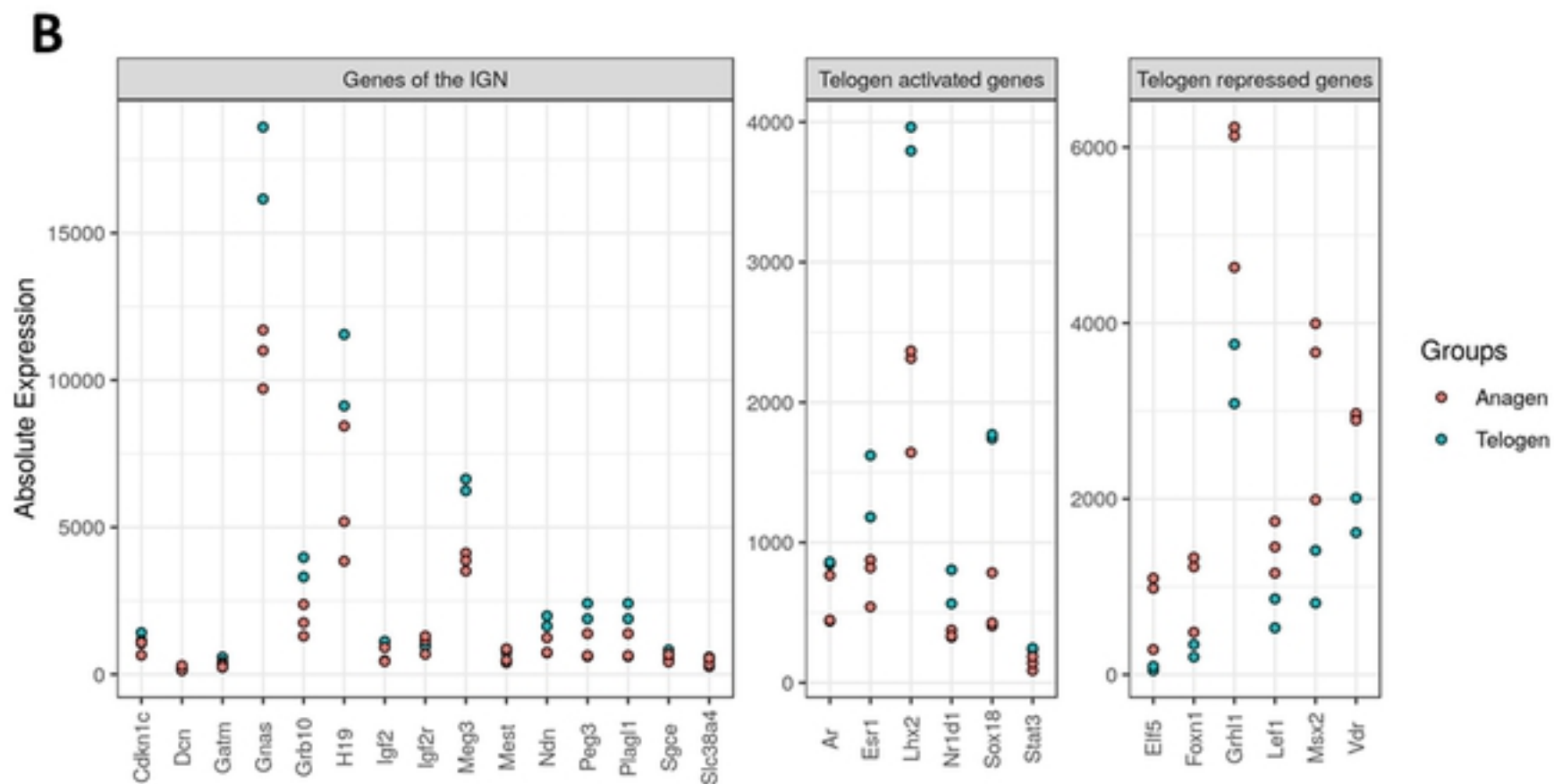
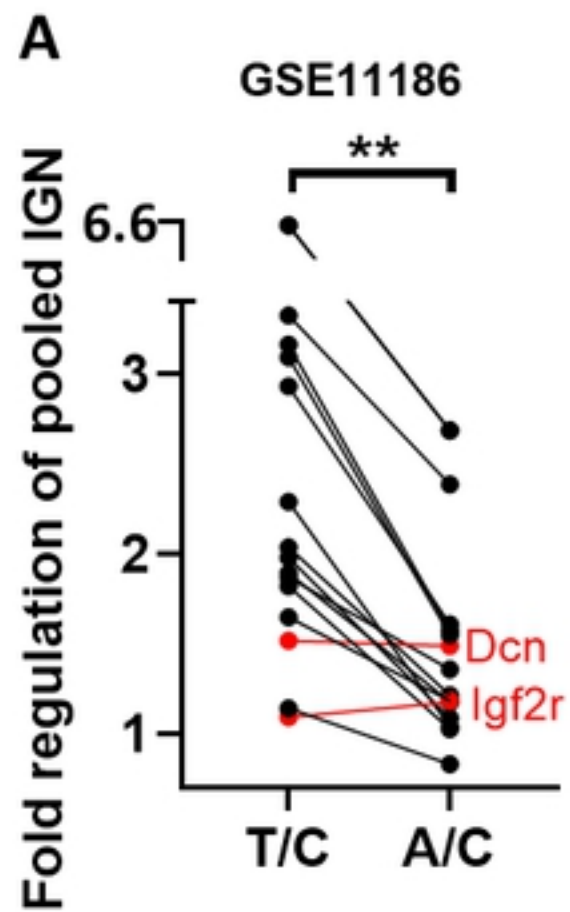
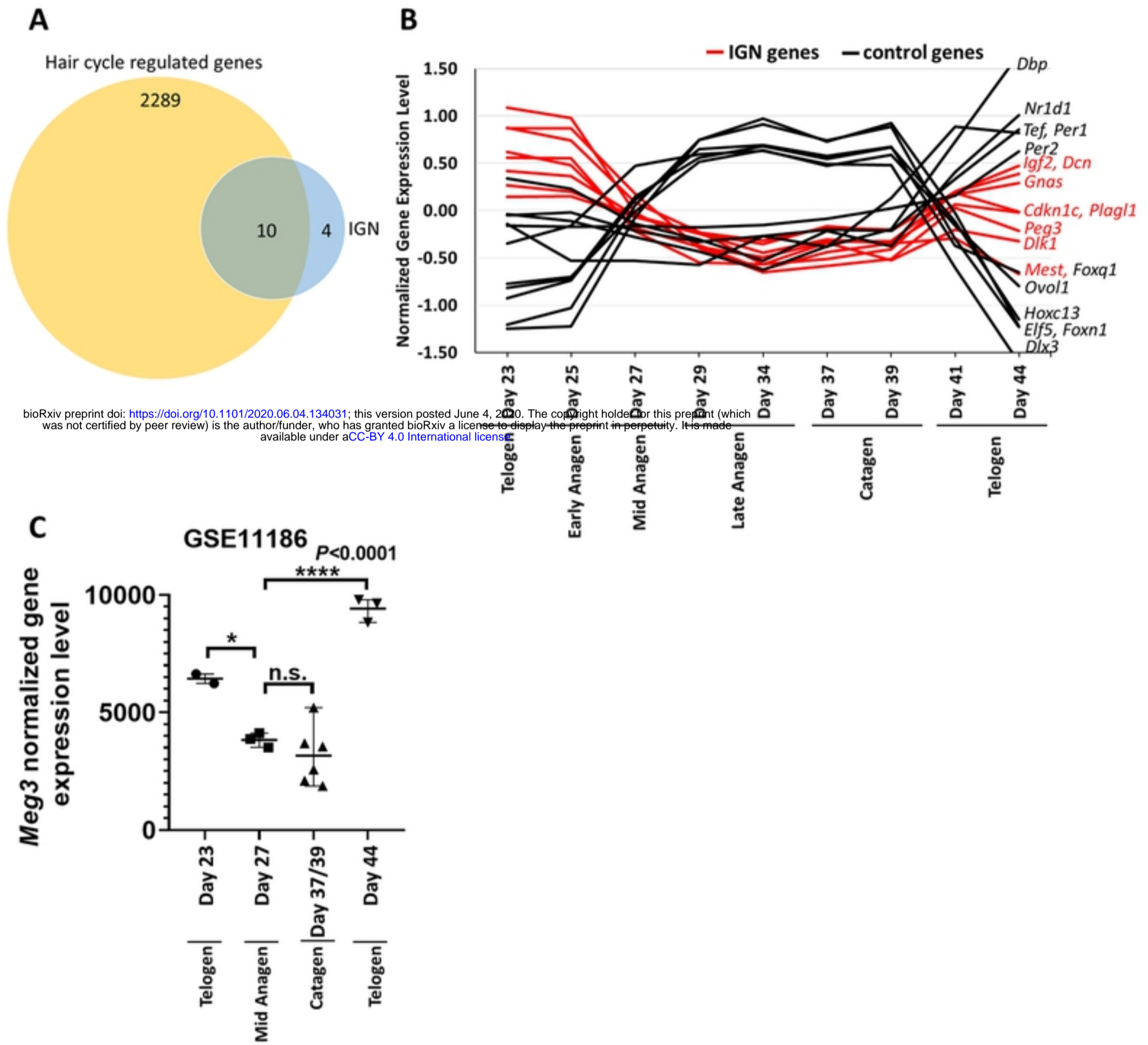


Figure 2



bioRxiv preprint doi: <https://doi.org/10.1101/2020.06.04.134031>; this version posted June 4, 2020. The copyright holder for this preprint (which was not certified by peer review) is the author/funder, who has granted bioRxiv a license to display the preprint in perpetuity. It is made available under aCC-BY 4.0 International license.

Figure 3